

# Cosmological Higgs-Axion Interplay for a Naturally Small Electroweak Scale

J.R. Espinosa<sup>a,b</sup>, C. Grojean<sup>a,b,c</sup>, G. Panico<sup>a</sup>, A. Pomarol<sup>d</sup>,  
O. Pujolàs<sup>a</sup>, G. Servant<sup>a,b,c,e</sup>

<sup>a</sup>*IFAE, Universitat Autònoma de Barcelona, 08193 Bellaterra, Barcelona, Spain*

<sup>b</sup>*ICREA, Institució Catalana de Recerca i Estudis Avançats, Barcelona, Spain*

<sup>c</sup>*DESY, Notkestrasse 85, 22607 Hamburg, Germany*

<sup>d</sup>*Dept. de Física, Universitat Autònoma de Barcelona, 08193 Bellaterra, Barcelona*

<sup>e</sup>*II. Institute of Theoretical Physics, University of Hamburg, D-22761 Hamburg, Germany*

## Abstract

Recently, a new mechanism to generate a naturally small electroweak scale has been proposed. It exploits the coupling of the Higgs to an axion-like field and a long era in the early universe where the axion unchains a dynamical screening of the Higgs mass. We present a new realization of this idea with the new feature that leaves no signs of new physics up to a rather large scale,  $10^9$  GeV, except for two very light and weakly coupled axion-like states. One of the scalars can be a viable Dark Matter candidate. Such a cosmological Higgs-axion interplay could be tested with a number of experimental strategies.

# 1 Introduction

Our understanding of Nature is based on the empirical evidence that natural phenomena taking place at different energy/distance scales do not influence each other. At present, these different phenomena are described by a succession of effective theories with different degrees of freedom manifesting themselves as shorter and shorter distances are probed. The parameters of the low-energy effective theory are *natural* if they do not require any special tuning of the parameters of the theory at higher energies.

Wilson [1] and 't Hooft [2] gave a quantitative meaning to this naturalness principle by demanding that all dimensionless parameters controlling the different effective theories should be of order unity unless they are associated to the breaking of a symmetry. Numerous examples of the naturalness principle to understand the necessity of new phenomena have been extensively discussed in the literature (see for instance [3] and references therein).

The Higgs boson mass and the value of the cosmological constant have been long recognized as two notorious challengers of this naturalness principle, a situation that stimulated the creativity of physicists in finding extensions of the Standard Model at higher energies. In most of these efforts to explain the smallness of the Higgs mass, such as supersymmetric and composite Higgs models, new physics is predicted to be present at TeV energies. Recently, however, a radically new approach to the Higgs mass hierarchy problem has been proposed [4], in reminiscence of the relaxation mechanism of [5] proposed for explaining dynamically the smallness of the cosmological constant (see [6, 7] for similar previous ideas). In principle, in this new approach no new degrees of freedom around the TeV scale are needed anymore to screen the Higgs mass from large quantum corrections. This has of course profound implications for the physics agenda of the LHC and beyond.

Technically, the relaxation mechanism of [4] is based on the cosmological interplay between the Higgs field  $h$  and an axion-like field  $\phi$ , arising from the following three terms of the scalar effective potential:

$$V(\phi, h) = \Lambda^3 g \phi - \frac{1}{2} \Lambda^2 \left( 1 - \frac{g\phi}{\Lambda} \right) h^2 + \epsilon \Lambda_c^4 \left( \frac{h}{\Lambda_c} \right)^n \cos(\phi/f) + \dots, \quad (1)$$

where  $\Lambda$  is the UV cut-off scale of the model, while  $\Lambda_c \lesssim \Lambda$  is the scale at which the periodic  $\cos(\phi/f)$ -term originates and  $n$  is a positive integer. The first term is needed to force  $\phi$  to roll-down in time, while the second one corresponds to a Higgs mass-squared term with a (positive) dependence on  $\phi$  such that different values of  $\phi$  scan the Higgs mass over a large range, including the weak scale. Finally, the third term plays the role of a potential barrier

for  $\phi$ , dependent on  $h$ , necessary to stop the rolling of  $\phi$  once electroweak symmetry breaking (EWSB) occurs. For this mechanism to work, it is also crucial to have a friction force, coming for example from Hubble friction during inflation, in order to make the rolling of  $\phi$  very slow to access the right minimum during the cosmological evolution. We will discuss the possible ultraviolet (UV) origin of Eq. (1) later on.

At the classical level, the proposed mechanism can be understood in the following way. Assuming that  $\phi$  starts, at the beginning of the inflationary epoch, at a very large value  $\phi \gtrsim \Lambda/g$ , it will slow-roll until it takes the critical value  $\phi_c = \Lambda/g$ , at which the Higgs mass-squared becomes zero. From this time on, as  $\phi$  continues slowly rolling down, the Higgs mass becomes negative, and it is energetically favored to turn on the Higgs field. This raises the third term of Eq. (1) up to the point at which  $\phi$  stops rolling. For  $g \ll 1$ , this occurs for a Higgs value  $v$  given by

$$g\Lambda^3 \simeq \frac{\Lambda_c^{4-n} v^n}{f} \epsilon. \quad (2)$$

This equation arises from demanding that the steepness of the linear  $\phi$ -term of the potential, first term of Eq. (1), equals the steepness of the Higgs barrier, third term of Eq. (1). From Eq. (2) we see that we can have  $v \ll \Lambda$  by taking  $g$  small enough, which is technically natural as  $g$  defines the spurion that breaks the symmetry  $\phi \rightarrow \phi + 2\pi f$ . At the quantum level, the described cosmological evolution is not much affected provided certain conditions, specified in [4] and discussed later, are fulfilled. Therefore, this mechanism potentially offers a new solution to the hierarchy problem. We will refer to this as the cosmological Higgs-axion interplay (CHAIN) mechanism.

For  $n = 1$ , the third term of Eq. (1) is linear in  $h$ , implying that  $\epsilon\Lambda_c^3$  must arise from a source of EWSB other than the Higgs. This can be the QCD quark-condensate  $\langle q\bar{q} \rangle \sim \Lambda_{QCD}^3$ , as proposed in [4]. In this case  $\Lambda_c \sim \Lambda_{QCD}$  and  $\epsilon \sim y_u$ , where  $y_u$  is the up-quark Yukawa. This model, however, predicts too large a value for the QCD  $\theta$ -angle, in conflict with neutron electric dipole moment constraints. A possible way to fix this problem was explained in [4], but it requires a low cut-off scale,  $\Lambda \lesssim 30 - 1000$  TeV. Alternatively, one could consider models in which the condensate comes from a new strongly-coupled sector, a la Technicolor, with  $\Lambda_c \sim \text{TeV}$ , or advocate the presence of an additional elementary Higgs doublet. This latter case however requires some extra symmetries to keep the second Higgs doublet light, as we discuss in Appendix B. These models predict extra physics carrying electroweak charges around the TeV scale that can be found in present or near-future experiments.

For  $n = 2$  on the contrary, the  $h^2 \cos(\phi/f)$  term in  $V(\phi, h)$  can arise from the electroweak-invariant term  $|H|^2 \cos(\phi/f)$ , where  $H$  is the Higgs doublet, and therefore no extra source

of EWSB is needed beyond the SM Higgs. As a result, these models can, in principle, allow for a larger new-physics scale beyond the SM (BSM). Nevertheless, at the quantum level, extra terms can be now induced beyond those shown in Eq. (1). Indeed, just by closing  $H$  in a loop, we expect, at  $O(\epsilon)$ , the terms

$$\epsilon\Lambda_c^4 \cos(\phi/f) \ , \quad \epsilon\Lambda_c^3 g\phi \cos(\phi/f) \ , \quad (3)$$

to be generated. These terms give a potential to  $\phi$  that, unless  $\Lambda_c \lesssim v$ , make it stop slow-rolling much before the Higgs turns on. Therefore, if we want the CHAIN mechanism to work, we must have again new physics not far away from the weak scale and therefore potentially visible in forthcoming experiments. It is important to notice that this new physics is not responsible for keeping the Higgs light, but for generating the periodic term of Eq. (1). In the particular model of this type discussed in [4], extra fermions were predicted at around the weak scale. An important drawback of this type of models is that they must address a “coincidence problem”: they must provide a BSM scale  $\Lambda_c$  that must lie around the weak scale with no a priori reason, as the weak scale is determined by Eq. (2).

The aim of our work is to offer an existence proof that it is indeed possible to devise a model that dynamically generates a large mass gap between the Higgs mass and the new physics threshold. The proposed model will not have a “coincidence problem” as the only new physics scale will be associated with  $\Lambda \sim \Lambda_c \gg v$ . For this to work, we need to make the terms of Eq. (3) smaller than the term  $\epsilon\Lambda^2|H|^2 \cos(\phi/f)$ . For this purpose, we will introduce another slow-rolling field,  $\sigma$ , coupled to  $\cos(\phi/f)$ . During its cosmological evolution,  $\sigma$  will take a value such that  $\sigma \cos(\phi/f)$  will cancel the terms of Eq. (3). When this occurs,  $\phi$  will be free to move, tracking  $\sigma$  downhill. Only when the  $h$ -dependent term turns on,  $\phi$  will stop tracking  $\sigma$  and reach the minimum fixed by Eq. (2). We will be able to push the cut-off scale up to  $\Lambda \sim 10^9 \text{ GeV}$ , providing the first example of a natural theory with such a large BSM scale. The only new states,  $\phi$  and  $\sigma$ , will have masses below the weak scale, but they will be very weakly coupled to the SM, making them very difficult to detect at present and future experiments. Interestingly, as we will see, they could provide the source of dark matter needed in the universe.

## 2 Double scanner mechanism

The key new ingredient of our proposal, with respect to [4], is a second scanning field, that we call  $\sigma$ . The full potential, up to terms of order  $\epsilon$ ,  $g_\sigma$  and  $g$ , is given by

$$V(\phi, \sigma, H) = \Lambda^4 \left( \frac{g\phi}{\Lambda} + \frac{g_\sigma\sigma}{\Lambda} \right) - \Lambda^2 \left( \alpha - \frac{g\phi}{\Lambda} \right) |H|^2 + \lambda |H|^4 + A(\phi, \sigma, H) \cos(\phi/f) , \quad (4)$$

where

$$A(\phi, \sigma, H) \equiv \epsilon \Lambda^4 \left( \beta + c_\phi \frac{g\phi}{\Lambda} - c_\sigma \frac{g_\sigma\sigma}{\Lambda} + \frac{|H|^2}{\Lambda^2} \right) , \quad (5)$$

with  $0 < g, g_\sigma, \epsilon \ll 1$ , while  $\alpha, \beta$  and  $c_\phi, c_\sigma$  are  $O(1)$  positive coefficients. We assume that all terms of Eq. (4) are generated at the cut-off scale  $\Lambda$ . For simplicity and clarity, we are only considering linear terms in  $g\phi/\Lambda$ , but we could have taken a generic function of  $g\phi/\Lambda$  with the only requirement that it is monotonically decreasing or increasing in a wide region of order  $\Lambda/g$  (and similarly for  $\sigma$  with  $g \rightarrow g_\sigma$ ).

From Eqs. (4) and (5), we see that  $\phi$  scans the Higgs mass, while  $\sigma$  scans  $A(\phi, \sigma, H)$ , the overall amplitude—the *envelope*—of the oscillating term. This dependence of  $A(\phi, \sigma, H)$  on  $\sigma$  is crucial for our CHAIN mechanism to work, while the other terms in Eq. (5) are added since, as we said, they are anyway generated at the quantum level (by loops of  $H$ ). The potential in Eq. (4) is stable under quantum corrections in the small-coupling limit ( $g, g_\sigma, \epsilon \ll 1$ ) we consider. A possible UV origin of the periodic term in Eq. (4) is given in Appendix A.

We will study the time evolution of  $\phi$ ,  $\sigma$  and  $H$  during the inflationary epoch. Inflation is needed, as in [4], to provide the friction that makes the fields slow-roll and reach the desired minimum. The time evolution of  $\sigma$  is quite trivial, as for  $\epsilon \ll 1$ , it simply slides down:

$$\sigma(t) = \sigma_0 - g_\sigma \Lambda^3 t / (3H_I) . \quad (6)$$

In the cosmological evolution of  $\phi$  we can distinguish four stages, depicted in Fig. 1, that we qualitatively describe next:

- I) At the start of inflation we assume  $\phi \gtrsim \Lambda/g$  and  $\sigma \gtrsim \Lambda/g_\sigma$  such that the Higgs mass-squared and the amplitude  $A$  are positive. The field  $\phi$  is stuck in some deep minimum coming from the  $A \cos(\phi/f)$  term of Eq. (4), while the Higgs field value is zero.
- II) As  $\sigma$  evolves down, the amplitude  $A$  decreases until the point at which for  $\phi$  the steepness of  $A \cos(\phi/f)$  is smaller than the slope coming from the linear term of Eq. (4),

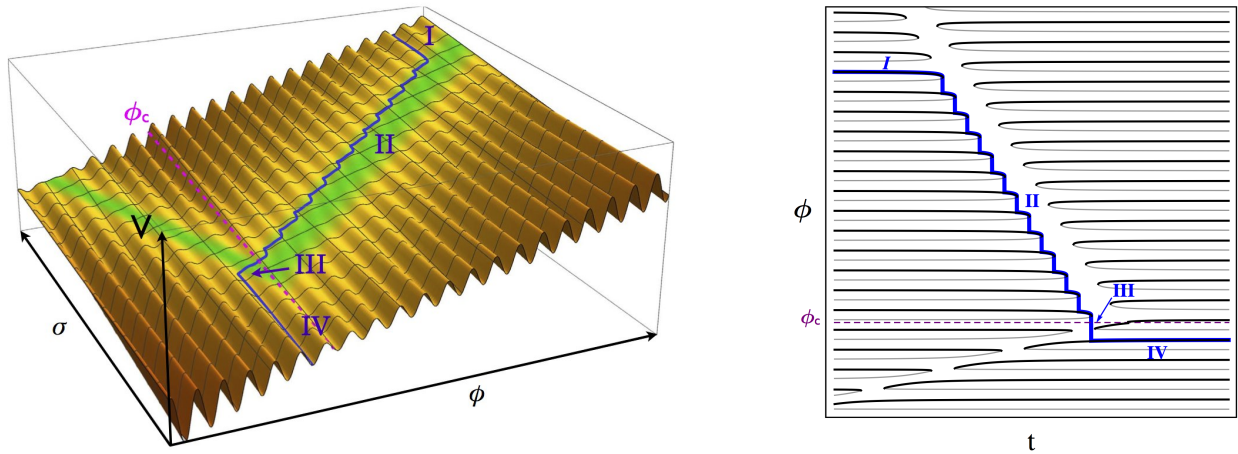


Figure 1: **Left:** Scalar potential in the  $\{\phi, \sigma\}$  plane. The band without barriers is in green while the barriers getting high(er) are dark(er) brown. The blue line shows a possible slow-roll cosmological trajectory of the fields during inflation. The dashed purple line is the critical line for EWSB. **Right:** Classical time evolution of  $\phi$  (blue curve) in the potential on the left. The black lines show the extremal points of the potential, with closely spaced minima (bold) and maxima (thin) alternating. (Arbitrary units and scales in both plots.)

and  $\phi$  can start to move down. The region in field-space at which this occurs is shown by a “green-band” in Fig. 1. In this region, the bumps from  $A \cos(\phi/f)$  are very small and, for  $g_\sigma \lesssim g$ ,  $\phi$  goes down tracking  $\sigma$ :  $\phi(t) \simeq \text{const.} + c_\sigma g_\sigma \sigma(t)/(c_\phi g)$ , which is the solution of  $A \approx 0$  (this solution neglects effects of size  $\Delta\phi \sim f$  which correspond to the stepwise behavior visible in Fig. 1).

- III) When  $\phi$  crosses the critical value  $\phi_c \equiv \alpha\Lambda/g$  the Higgs mass-squared term becomes negative, turning on  $H$ . This gives, according to Eq. (5), a positive contribution to the amplitude  $A$ , that, for certain values of the parameters of Eq. (4) to be specified later, makes the direction of the green-band change as shown in Fig. 1. The field  $\phi$  cannot continue any longer its evolution along the tracking trajectory that would bend in the opposite direction in  $\sigma$  and would not be compatible with the cosmological evolution of  $\sigma$  that imposes  $d\sigma/dt < 0$ . So  $\phi$  crosses the green-band.

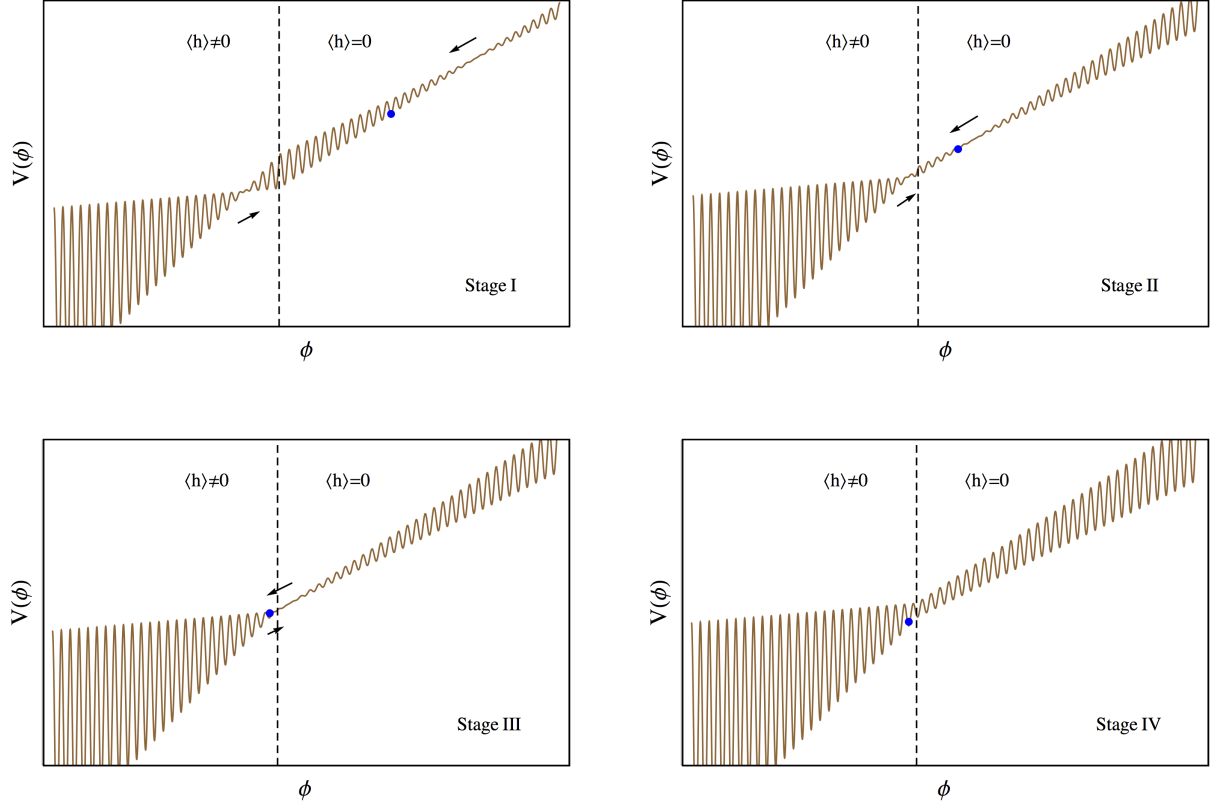


Figure 2: *Sketch of the four stages in the evolution of  $\phi$ , marked by the blue dot, in the time-dependent effective potential for  $\phi$  obtained after integrating out  $\sigma$  and  $H$  but corresponding to the same potential as in Fig. 1. (Arbitrary units and scales.)*

IV) Finally,  $\phi$  reaches the other side of the green-band (where  $A$  becomes large again) and gets stuck in a minimum from  $A \cos(\phi/f)$  as in the model of [4]. The field  $\sigma$  continues going down, making  $A$  grow until  $\sigma$  finds its own minimum.

For the same potential shown in Fig. 1, we show in Fig. 2 four snapshots of how  $\phi$  evolves in the time-dependent potential  $V(\phi) \equiv V(\phi, \sigma(t), h(\phi))$ , obtained after integrating out  $\sigma$  and  $h$ . We are choosing four representative time values corresponding to the four stages I-IV. At the stage I and II, this potential has two  $A \approx 0$  regions moving towards each other (as indicated by the arrows), that merge at stage III and disappear at stage IV.

To understand under which conditions the potential of Eq. (4) has the shape shown in

Fig. 1, we start by finding the  $\phi$  values, called  $\phi_*$ , for which the steepness from  $A \cos(\phi/f)$  is smaller than the steepness from the  $\Lambda^3 g \phi$  term of Eq. (4). These are determined by

$$\frac{1}{f} A(\phi_*, \sigma, h(\phi_*)) \lesssim g \Lambda^3, \quad (7)$$

where we are working in the limit  $g, g_\sigma \ll 1$ . In this range of  $\phi$  values,  $\partial V / \partial \phi = 0$  has no solutions, leading to a “sliding” region, the minima-free green-band of Fig. 1.

The value of the neutral Higgs component,  $\langle H \rangle = (0, h/\sqrt{2})$ , depends on  $\phi$  according to<sup>1</sup>

$$h^2(\phi) \simeq \frac{\Lambda^2}{\lambda} \left( \alpha - \frac{g\phi}{\Lambda} \right), \text{ for } \phi < \phi_c, \quad (8)$$

and zero otherwise. Solving Eq. (7), we obtain the interval(s)

$$\phi_* \in \begin{cases} \phi_c + \frac{c_\sigma g_\sigma}{c_\phi g} (\sigma - \sigma_c) \pm \frac{f}{c_\phi \epsilon}, & (\text{for } \phi_* > \phi_c) \\ \phi_c + \frac{c_\sigma g_\sigma}{c'_\phi g} (\sigma - \sigma_c) \pm \frac{f}{c'_\phi \epsilon}, & (\text{for } \phi_* < \phi_c), \end{cases} \quad (9)$$

with  $c'_\phi = c_\phi - 1/(2\lambda)$ . By continuity, both solutions merge at  $\phi_* = \phi_c$  at a particular value  $\sigma_c = (g c_\phi \phi_c + \beta \Lambda) / (c_\sigma g_\sigma)$ .<sup>2</sup>

In order for  $\phi(t)$  to track down  $\sigma(t)$ , or what is equivalent, for  $\phi(t)$  to stay in the  $\phi_*$  region of Eq. (9) until reaching  $\phi_c$ , the gradient of the dynamical trajectory in the  $\{\phi, \sigma\}$  plane<sup>3</sup> inside the  $\phi_*$  interval,

$$\frac{d\phi(t)/dt}{d\sigma(t)/dt} = \frac{g}{g_\sigma}, \quad (10)$$

should be larger than the gradient  $d\phi_*/d\sigma$  of the green-band itself. Otherwise  $\phi(t)$  crosses the green-band too early and gets stuck at some minimum before getting to  $\phi_c$ . From Eq. (9), this condition,  $d\phi(t)/d\sigma(t) > d\phi_*/d\sigma$ , leads to the requirement

$$c_\phi g^2 > c_\sigma g_\sigma^2. \quad (11)$$

On the contrary, once  $\phi \leq \phi_c$  we must demand  $\phi$  to exit the green-band (getting trapped in some vacuum precisely as needed to explain the smallness of the electroweak scale) which

---

<sup>1</sup>To simplify the discussion, we are ignoring a term  $-(\epsilon \Lambda^2 / \lambda) \cos(\phi/f)$  in the RHS of Eq. (8), that causes a transitory period in which the Higgs mass term switches sign repeatedly before stabilizing as negative.

<sup>2</sup>In fact, the kink in the sliding-band is located around the point  $\{\phi_c, \sigma_c\}$ . In terms of these coordinates one has  $A = \epsilon \Lambda^3 [c_\phi g(\phi - \phi_c) - c_\sigma g_\sigma(\sigma - \sigma_c) + |H|^2 / \Lambda]$ .

<sup>3</sup>Inside the  $\phi_*$  interval, we have  $A \approx 0$  and  $\phi$ 's slow-roll is driven by the linear term of Eq. (4).



implies  $d\phi(t)/d\sigma(t) < d\phi_*/d\sigma$  and leads to

$$c'_\phi g^2 < c_\sigma g_\sigma^2. \quad (12)$$

This condition is easily satisfied for  $c'_\phi < 0$ , which is equivalent to  $2\lambda c_\phi < 1$ , and corresponds to the situation depicted in Fig. 1 in which the green-band flips direction at  $\phi = \phi_c$ . For  $2\lambda c_\phi > 1$ , the green-band does not switch direction at  $\phi_c$  but its slope changes. This occurs however for a small range of  $c_\phi$  where Eq. (12) is also fulfilled:

$$\frac{1}{2\lambda} < c_\phi < \frac{1}{2\lambda} + \frac{c_\sigma g_\sigma^2}{c_\phi g^2}. \quad (13)$$

This region of the parameter space can then also provide an explanation to the smallness of the electroweak scale.

Let us emphasize that the CHAIN mechanism described above works independently of  $\phi_i$ , the initial condition for  $\phi$ , provided only that  $\phi_i$  at the initial time  $t_i$  lies in the region  $\phi_c < \phi_i < \phi_*(t_i)$ , which is a natural and sizable range of the available field space. A  $g_\sigma \sigma |H|^2$  term in the potential could spoil the CHAIN mechanism, as the late evolution of  $\sigma$ , after  $\phi$  is settled in its minimum, would change the value of the Higgs mass. Therefore we find that this term, if present, must be further suppressed by an extra factor  $\epsilon$ . This does not pose any problem to our model as a radiatively generated  $\sigma |H|^2$  term arising from Eq. (4) by loops of  $\phi$ , is indeed very small, of  $O(\epsilon^2 g_\sigma)$ .

### 3 Consistency requirements for a small weak scale

The potential in Eq. (4) involves two scales,  $\Lambda$  and  $f$ , and three small couplings,  $g, g_\sigma$  and  $\epsilon$ , apart from a few dimensionless parameters of order unity (including the Higgs quartic coupling,  $\lambda$ ). The cosmological evolution of our model can be broadly described by these parameters and two external quantities fixed by the inflaton sector:  $H_I$ , the value of the Hubble parameter during inflation, and  $N_e$ , the number of  $e$ -folds. These various parameters have to satisfy several constraints in order to provide a natural solution to the hierarchy problem, i.e., to dynamically ensure a stable separation between the weak scale and the high-energy scale  $\Lambda$  from which the potential Eq. (4) emerges as a low-energy description. These constraints arise from demanding

1. *Dangerous quantum corrections to the potential are kept small.* At least at the quantum level, additional terms of  $O(\epsilon^2)$  can be generated in the potential of Eq. (4) that could

potentially spoil our CHAIN mechanism. For instance, terms like<sup>4</sup>  $\epsilon^2 \Lambda^4 \cos^2(\phi/f)$  or  $\epsilon^2 \Lambda^3 g \phi \cos^2(\phi/f)$ , depend quadratically on  $\cos(\phi/f)$ , and therefore their amplitudes cannot be cancelled by  $\sigma$  simultaneously to  $A \cos(\phi/f)$ . These terms are dangerous since they give a barrier to  $\phi$  at values that can be above the critical  $\phi_c$ . To make sure that they remain subdominant to the Higgs barrier of Eq. (4), we must demand

$$\epsilon \lesssim v^2/\Lambda^2. \quad (14)$$

This condition also ensures that the contribution to the Higgs mass coming from the  $\epsilon \Lambda^2 |H|^2 \cos(\phi/f)$  term in the potential is at most of electroweak size and does not spoil the tracking behaviour (see footnote 1).

2.  *$\phi$  must be trapped by the Higgs barrier.* As in the model of [4], the nonzero Higgs field must be the only one responsible for stopping  $\phi$  from sliding any longer. This is the requirement in Eq. (2) that, for our case  $n = 2$  and  $\Lambda = \Lambda_c$ , reads  $g \Lambda^3 \simeq \epsilon \Lambda^2 v^2/f$ . This can be used to obtain the electroweak scale as a prediction from the model in terms of microscopic parameters:

$$v^2 \simeq \frac{g \Lambda f}{\epsilon}. \quad (15)$$

We will also use this relation later on to get rid of  $\epsilon$  in terms of the other parameters of the model, so that the electroweak scale is reproduced correctly.

3. *Inflation is independent of the  $\phi$  and  $\sigma$  evolution.* We assume for simplicity that inflation is driven by another field, the inflaton, that does not receive any back-reaction from the evolution of  $\phi$  and  $\sigma$ . This is possible under the condition that the typical energy density carried by  $\phi$  and  $\sigma$  remains smaller than the inflation scale, i.e.,

$$\frac{\Lambda^2}{M_P} \lesssim H_I, \quad (16)$$

where  $M_P$  is the reduced Planck mass,  $M_P \simeq 2.4 \times 10^{18}$  GeV.

4. *Classical rolling dominates over quantum jumping.* We are assuming that the cosmological evolution of  $\phi$  and  $\sigma$  is dominated by classical physics. It is therefore essential, for the consistency of our solution, that during the cosmological evolution of our system the quantum fluctuations of the fields, typically of size  $H_I$ , remain smaller than the

---

<sup>4</sup>See Appendix A for the possible origin of these terms in a particular UV completion.

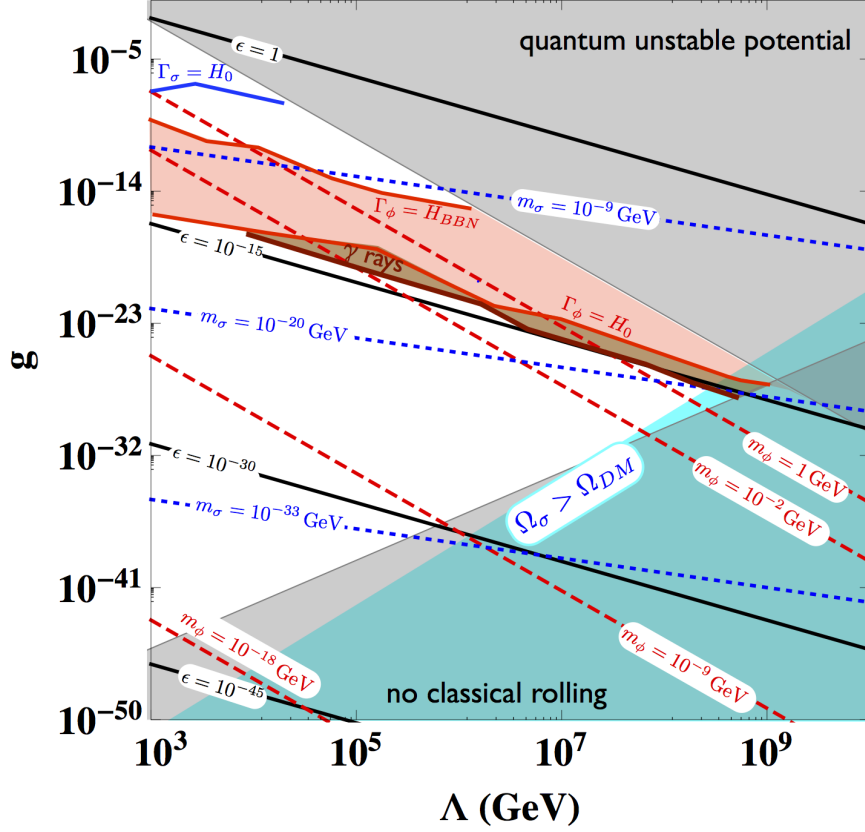


Figure 3: *Parameter space for a successful solution of the hierarchy problem ensured by the cosmological evolution of the fields  $\phi$  and  $\sigma$ . We have taken  $\Lambda = f$  and  $g_\sigma = 0.1g$ . In the upper shaded gray region, the quantum corrections to the potential would not drive the system towards the weak scale while in the lower shaded gray region, the two fields would not follow their classical paths. Some contour lines of the expansion parameter  $\epsilon$  (continuous black) and of the physical masses of  $\sigma$  (dotted blue) and  $\phi$  (dashed red) are reported. In the shaded red region, the field  $\phi$  decays after BBN and has a lifetime shorter than the age of the universe. The brown shaded region is excluded by gamma-ray data. Finally, in the shaded cyan region on the bottom right corner, the energy density stored in the oscillations of the field  $\sigma$  exceeds the DM energy density.*

classical field displacements over one Hubble time, i.e.,  $\Delta\sigma \sim H_I^{-1} d\sigma/dt \sim H_I^{-2} dV/d\sigma$

for the case of  $\sigma$ . This condition for classical rolling [4] simply reads

$$H_I^3 \lesssim g_\sigma \Lambda^3, \quad (17)$$

for  $\sigma$ . Due to Eq. (11), the classical-rolling condition for  $\phi$  is automatically guaranteed whenever Eq. (17) is fulfilled (we assumed that  $c_\phi \sim c_\sigma \sim 1$ ).

5. *Inflation lasts long enough for complete scanning.* In order for the above mechanism to work for generic initial field configurations, it is essential that the range scanned by  $\phi$  and  $\sigma$  during inflation be of order or larger than  $\Lambda/g$  and  $\Lambda/g_\sigma$  respectively. This is ensured by requiring a long enough period of inflation, namely,  $N_e \Delta\sigma \sim N_e H_I^{-2} dV/d\sigma \gtrsim \Lambda/g_\sigma$ , which leads to

$$N_e \gtrsim \frac{H_I^2}{g_\sigma^2 \Lambda^2}. \quad (18)$$

The typical duration of the different stages of the cosmological evolution of  $\phi$  is of the same order, with the exception of stage III, which is much shorter, of order  $N_e^{III} \sim (gf/\epsilon\Lambda)N_e$ .

Combining these various consistency conditions, together with Eq. (11), we obtain that the couplings  $g_\sigma$  and  $g$  are bounded to the interval:

$$\frac{\Lambda^3}{M_P^3} \lesssim g_\sigma \lesssim g \lesssim \frac{v^4}{f\Lambda^3}. \quad (19)$$

Since  $f$  cannot be much smaller than  $\Lambda$ , as this latter is the scale at which the  $\cos(\phi/f)$  term is generated, we obtain from Eq. (19) an upper bound on the cut-off of our model:

$$\Lambda \lesssim (v^4 M_P^3)^{1/7} \simeq 2 \times 10^9 \text{ GeV}. \quad (20)$$

The bound in Eq. (19) defines the region of the parameter space of the model consistent with a natural solution to  $v \ll \Lambda$ . This is shown in Fig. 3, where, for concreteness, we have taken  $f = \Lambda$  and  $g_\sigma = 0.1g$ .

## 4 Quantum spreading

The discussion of the cosmological evolution in Section 2 was fully classical. As we saw in more detail in the previous Section, the model parameters can be chosen to ensure that

the slow-roll of the fields  $\phi$  and  $\sigma$  is indeed dominated by classical evolution, with quantum fluctuations (driven by  $H_I$ ) playing a subdominant role. As discussed in [4], however, one should pay attention to the subleading quantum spreading to ensure that it does not spoil the solution to the hierarchy problem.

This issue can be attacked using a Langevin equation (that adds to the usual classical evolution of the field a noise term that captures the random fluctuations controlled by  $H_I$ ) or using the Fokker-Planck equation<sup>5</sup>

$$\frac{\partial P}{\partial N_e} = \frac{\partial}{\partial \phi} \left( \frac{P}{3H_I^2} \frac{\partial V}{\partial \phi} \right) + \frac{\partial^2}{\partial \phi^2} \left( \frac{H_I^2}{8\pi^2} P \right) , \quad (21)$$

for  $P(\phi, N_e)$  the probability (density) of finding the field in the interval  $(\phi, \phi + d\phi)$  in a given Hubble patch after  $N_e$   $e$ -folds of inflation. The first term in the equation describes the effect of classical slow roll while the second describes the quantum fluctuations induced by inflation.

It is convenient to define the average value of  $\phi$ ,  $\langle \phi \rangle$ , and its variance  $\Delta\phi^2 = \langle (\phi - \langle \phi \rangle)^2 \rangle$ , where

$$\langle F(\phi) \rangle \equiv \int_{-\infty}^{\infty} P(\phi, N_e) F(\phi) d\phi . \quad (22)$$

Using the Fokker-Planck Eq. (21), one gets

$$\frac{d\langle \phi \rangle}{dN_e} = -\frac{1}{3H_I^2} \left\langle \frac{\partial V}{\partial \phi} \right\rangle , \quad (23)$$

$$\frac{d\Delta\phi^2}{dN_e} = \frac{H_I^2}{4\pi^2} - \frac{2}{3H_I^2} \left\langle (\phi - \langle \phi \rangle) \frac{\partial V}{\partial \phi} \right\rangle . \quad (24)$$

The first equation shows that  $\langle \phi \rangle$  slow-rolls classically down an averaged potential slope. The second equation describes the quantum spread of the field. Besides the positive contribution that makes the variance grow with  $H_I$ , as  $\Delta\phi \sim \sqrt{N_e} H_I$ , there is an effect from the potential that can eventually stop the quantum spreading (*e.g.* in a potential well).

We can use these equations to gain some qualitative understanding of how the field  $\phi$  will spread during its cosmological evolution (described in Section 2). During stage I,  $\phi$  is stuck in a deep minimum where we can neglect quantum spreading effects. In stage II,  $\phi$  rolls at the bottom of the  $\phi_*$  range and it is a good approximation to assume that  $\langle \phi \rangle \sim (\phi_*)_{\min}$ , the low end of the  $\phi_*$  region. The potential around that point is asymmetric, with a nearly constant and very small slope in the  $\phi_*$  range and a steeper slope outside that range (the

---

<sup>5</sup>For more details on the use of these equations to describe fluctuating light fields (like the Higgs) during inflation, see *e.g.* [8].

hilly side that actually slows down the field so that it tracks  $(\phi_*)_{\min}$ . As a result, the spread of  $\phi$  is also asymmetric, being suppressed in the hilly side and larger inside the  $\phi_*$  range. The latter spread starts growing at the beginning of stage II and, depending on how large  $H_I$  is and how long stage II lasts, it might reach a steady state (with  $d\Delta\phi^2/dN_e \simeq 0$ ). Irrespective of that, it is guaranteed that the final quantum spread will be at most of the same order of the size of the  $\phi_*$  region ( $\Delta\phi_* = f/(c_\phi\epsilon) \sim f/\epsilon$ ) because the large barriers beyond that range suppress the spreading.<sup>6</sup> How far away from the  $\phi_*$ -region the barriers will stop the spreading can be estimated (by comparing the classical falling speed with the uphill quantum jumps) as

$$\delta\phi \sim \frac{f}{\epsilon} \times \frac{H_I^3}{g\Lambda^3}, \quad (25)$$

which is the width of the band times a factor smaller than 1, see Eq. (17). The same applies to stage III, with a similar bound on the final spread  $\Delta\phi \lesssim f/\epsilon$ . In terms of the Higgs field expectation value, using Eq. (8), this translates into an spread of the order  $g f \Lambda / (2\lambda\epsilon)$ , which is of the order of  $v^2$  as we saw in the previous Section, Eq. (15). So the mechanism to solve the hierarchy problem is not spoiled. As in [4], our modified CHAIN mechanism does not offer a solution to the cosmological constant problem.

Quantum spreading will also affect the field  $\sigma$ , which rolls down a much simpler potential. Its spread will grow as  $\Delta\sigma \sim \sqrt{N_e} H_I$  and its final value at the end of inflation will depend on the shape of the potential near the final  $\sigma$  minimum. Concerning the evolution of the field  $\phi$ , the spreading of  $\sigma$  will not matter (as long as classical rolling dominates):  $\phi$  will simply track  $\sigma$  wherever it is in a given Hubble patch.

## 5 Cosmological signatures

As we saw in the previous Sections, in contrast with the models of Ref. [4], the new-physics scale of our model can be as large as  $\Lambda \sim 10^9$  GeV, and therefore we do not expect any new state around the weak scale. Only the two additional scalars  $\sigma$  and  $\phi$  are lighter than, or at most around, the weak scale. However, as we will see below, they are very weakly-coupled to

---

<sup>6</sup>There is always a small probability that the field leaks to neighbouring minima (with the overall slope biasing the leakage towards lower minima) but the exponential suppression ( $\sim \exp[-8\pi^2 V/(3H_I^4)]$ ) of the process overcomes the large number of e-folds in stage IV. Notice also that the minimum at which  $\phi$  ends up is extremely stable against decay by quantum tunneling after inflation is over. The tunneling bounce action can be estimated (in the thin-wall approximation) to be  $S_4 \sim \epsilon^2 f / (\Lambda g^3) \gtrsim (\Lambda/v)^8$ , which leads to a vacuum lifetime many orders of magnitude larger than the age of the universe.

the SM states in most of the parameter space, and thus can only have some phenomenological impact through astrophysical and cosmological effects.

## 5.1 Properties of $\phi$ and $\sigma$

We start by deriving the properties of the  $\phi$  and  $\sigma$  scalars. After the slow-rolling process ends and  $\sigma$  settles in a minimum, no cancellation is expected in the  $A(\phi, \sigma, H)$  amplitude, so that  $A(\phi, \sigma, H) \sim \epsilon \Lambda^4$ . The mass of  $\phi$  is thus controlled by  $A \cos(\phi/f)$  and can be estimated as

$$m_\phi^2 \sim \frac{\epsilon \Lambda^4}{f^2} \sim g \frac{\Lambda^5}{f v^2} \lesssim v^2, \quad (26)$$

where we used Eq. (14) and Eq. (15) to obtain the second equality and the upper bound on  $m_\phi$ . For  $\sigma$  we expect that higher-order terms in  $g_\sigma \sigma / \Lambda$ , not shown for simplicity in Eq. (4), give it a mass of order

$$m_\sigma^2 \sim g_\sigma^2 \Lambda^2 \ll m_\phi^2. \quad (27)$$

In the allowed part of the parameter space of our model the masses of the two scalars can change by many orders of magnitude, spanning the range  $[10^{-20}, 100]$  GeV for  $\phi$  and  $[10^{-45}, 10^{-2}]$  GeV for  $\sigma$ . Contours of constant  $m_\phi$  and  $m_\sigma$  are shown in Fig. 3.

These two scalars interact with the SM particles mainly through a mass mixing with the Higgs. The corresponding mixing angles can be estimated as

$$\theta_{\phi h} \sim \frac{g \Lambda v}{m_h^2}, \quad \theta_{\sigma \phi} \sim \frac{g_\sigma f v^2}{\Lambda^3}, \quad \theta_{\sigma h} \sim \text{Max} \left\{ \theta_{\sigma \phi} \theta_{\phi h}, \frac{g^2}{16 \pi^2} \frac{g_\sigma \Lambda^7}{f^2 v^3 m_h^2} \right\}. \quad (28)$$

Notice that the  $\phi - h$  mass mixing coming from  $\partial_{\phi h}^2 V \sim \epsilon \Lambda^2 (v/f) \sin(\phi/f)$  is suppressed at the minimum where we have  $\sin(\langle \phi \rangle / f) \sim g f / (\epsilon \Lambda) \sim v^2 / \Lambda^2 \ll 1$ .<sup>7</sup> The first contribution in  $\theta_{\sigma h}$  arises at tree-level, whereas the second one originates from a  $\phi$ -loop. For most of the parameter space we consider, this loop term dominates over the tree level one. The scalar potential Eq. (4) also gives rise to interactions between  $\phi$  and the Higgs, not suppressed by the small mixing angle  $\theta_{\phi h}$ , that are of order

$$\phi \phi h h : \quad \epsilon \Lambda^2 / f^2, \quad \phi \phi h : \quad \epsilon v \Lambda^2 / f^2, \quad (29)$$

---

<sup>7</sup>This is to be contrasted with the beginning of Phase IV when  $\sin(\phi/f) \sim 1$ , as used to derive Eq. (15), since barriers are smaller at this earlier stage. At the end of Phase IV the barriers have grown large, and  $\phi$  is close to the minimum of its cosine potential.

and will play an important role in the thermal production of  $\phi$ . The decays of  $\phi$  and  $\sigma$  are mediated by the mixing with the Higgs, and thus the widths are given by

$$\Gamma_\phi \sim \theta_{\phi h}^2 \Gamma_h(m_\phi), \quad \Gamma_\sigma \sim \theta_{\sigma h}^2 \Gamma_h(m_\sigma), \quad (30)$$

where  $\Gamma_h(m_i)$  is the SM Higgs width evaluated at  $m_h = m_i$ . Contours for  $\Gamma_{\phi,\sigma}$  are shown in Fig. 3 (the values of the width  $\Gamma_h(m_i)$  are subject to large theoretical uncertainties in the mass region around 1 GeV where several hadronic decay channels open up [9]; we used the expressions given in Ref. [10] –see also Refs. [11, 12]). For masses below  $2m_e \sim 1$  MeV, we have  $\Gamma_h(m_i) \sim (m_i/m_h)^3 \Gamma_{h \rightarrow \gamma\gamma}(m_h)$ , and therefore, in a major part of the parameter space,  $\phi$  and  $\sigma$  have suppressed decay widths controlled by the decay into photon pairs. As shown in Fig. 3, there is a sizable part of the parameter space in which  $\phi$  is cosmologically unstable ( $\Gamma_\phi > H_0$ , where  $H_0$  is the present Hubble value), but sufficiently long-lived to decay after Big Bang Nucleosynthesis (BBN) ( $\Gamma_\phi < H_{BBN} \equiv H(T = 1 \text{ MeV})$ ). As we will see in the following, this region of the parameter space can be constrained by cosmology. On the other hand,  $\sigma$  is cosmologically stable in most of the relevant parameter space, and can decay within the age of the universe only in a small corner of the parameter space, namely for  $g_\sigma \gtrsim 10^{-8}$  and  $\Lambda \lesssim 10^4$  GeV.

We can now easily estimate the cosmological abundances of  $\phi$  and  $\sigma$ , either stored in late classical oscillations (vacuum misalignment) or from thermal production. This will allow us to set bounds on the model from overclosure of the universe, post-BBN decays or astrophysical constraints.

## 5.2 Impact of $\phi$ and $\sigma$ on standard cosmological predictions

In this work we assume for simplicity that, once both  $\phi$  and  $\sigma$  have settled in their minima, inflation ends with an unspecified reheating period. We will assume a reheating temperature higher than the EW scale in what follows.

### Abundances of $\phi$ and $\sigma$ from vacuum misalignment

If after inflation and reheating, the fields  $\phi$  and  $\sigma$  end up displaced from their minima, they will fall towards them, oscillating around them if their lifetimes are large. The energy density stored in the field oscillations behaves like cold dark matter and can potentially overclose the universe today or dissociate light elements if the decay takes place during or after BBN. At the start, the field energy density is dominated by the potential energy, but



as the fields roll to their minima and pick up speed, the kinetic energy grows. When both contributions are of similar size, one can properly talk about oscillating fields. This happens for the Hubble value  $H \lesssim m_i$  ( $i = \phi, \sigma$ ) or, equivalently, in a radiation-dominated universe, at  $T_{osc}^i \sim \sqrt{m_i M_P}$ . In that oscillating regime, the energy density scales as that of non-relativistic matter,  $\rho_i(T) \sim \rho_{ini}^i (T/T_{osc}^i)^3$ , where  $\rho_{ini}^i$  is the initial amount of energy at the start of the oscillating regime (this is smaller than the original potential energy density, but only by an order one factor).

Let us start considering the  $\sigma$  field. We expect that during inflation  $\sigma$  slowly rolled down to its global minimum, somewhere in its  $\sim \Lambda/g_\sigma$  range, as this requires a number of e-folds similar to the  $N_e$  estimated in Eq. (18). Because of quantum effects (see Section 4),  $\sigma$  reached the minimum with a spread  $\sqrt{N_e} H_I$ . We can use this result to estimate the typical displacement from the minimum at the end of inflation:

$$(\Delta\sigma)_{ini} \sim \sqrt{N_e} H_I .$$

This displacement is quite large though still smaller than  $\Lambda/g_\sigma$ , and hence we can estimate the amount of energy density as  $\rho_{ini}^\sigma \sim m_\sigma^2 (\Delta\sigma)_{ini}^2$ . Using  $N_e \sim H_I^2/(\Lambda^2 g_\sigma^2)$ , we finally get  $\rho_{ini}^\sigma \sim H_I^4$ . The energy density stored in  $\sigma$  oscillations today, relative to the critical energy density, is then, using Eq. (16),  $\Omega_\sigma \gtrsim (4 \times 10^{-27}/g_\sigma)^{3/2} (\Lambda/10^8 \text{ GeV})^{13/2}$ . The bound to avoid universe overclosure ( $\Omega_\sigma \lesssim 1$ ), translates into

$$g_\sigma \gtrsim 4 \times 10^{-27} \left( \frac{\Lambda}{10^8 \text{ GeV}} \right)^{13/3} . \quad (31)$$

The contour  $\Omega_\sigma = \Omega_{DM}$  is plotted in Fig. 3, limiting the excluded blue region. It shows that  $\sigma$  can be a good dark matter candidate in the region where the bound (31) is saturated, in particular at large  $\Lambda$ . For certain values of  $m_\sigma$ , there can be other cosmological constraints. For example, for  $\Omega_\sigma \gtrsim \Omega_{DM}/20$ , the mass range  $10^{-32} \text{ eV} \lesssim m_\sigma \lesssim 10^{-25.5} \text{ eV}$  is excluded by structure formation [20], while masses around  $m_\sigma \sim 10^{-11} \text{ eV}$  may be constrained by Black Hole superradiance [14]. Interestingly, for the particular case  $m_\sigma \sim 10^{-24} \text{ eV}$ ,  $\sigma$  could be searched for by the SKA pulsar timing array experiment [19]. Let us finally notice that there are ways to go around the bound (31), for instance, by assuming a late entropy production after  $\sigma$  has started to oscillate, as can occur if reheating is a very slow process such that  $T_{RH} < T_{osc}^\sigma$  [13].

The situation for  $\phi$  is rather different. At the end of its evolution,  $\phi$  is trapped in a region with high barriers and its displacement from the minimum originates from the

possible quantum spreading. The initial energy density arising from this displacement was at most  $\rho_{ini}^\phi \sim H_I^4$ , that, since  $m_\phi \gg m_\sigma$  and then  $T_{osc}^\phi \gg T_{osc}^\sigma$ , gives today a completely negligible effect.

### Thermal production of $\phi$

Thermal production of  $\phi$  arises mainly from the couplings of Eq. (29). In particular, from the  $\phi\phi hh$ -coupling we can have double-production from the thermal bath via  $h+h \rightarrow \phi+\phi$ .<sup>8</sup> At  $T \gtrsim m_h$ , this double-production cross-section is estimated to be  $\langle\sigma_{AV}\rangle \sim \epsilon^2(\Lambda^4/f^4)/T^2$ . This implies that  $\phi$  can reach thermal equilibrium only for  $T$  in the interval  $[m_h, \epsilon^2 M_P(\Lambda/f)^4]$ , in which the  $\phi$  production rate is faster than the rate of expansion. This region corresponds roughly to the area above the  $\Gamma_\phi = H_{BBN}$  line of Fig. 3, so we conclude that in most of the parameter space,  $\phi$  never thermalizes.<sup>9</sup>

The number density of  $\phi$  produced thermally is obtained by solving the Boltzmann equation

$$\frac{dn_\phi}{dt} + 3Hn_\phi = -\langle\sigma_{AV}\rangle(n_\phi^2 - n_{\phi,eq}^2), \quad (32)$$

where  $n_{\phi,eq}$  is the equilibrium number-density of  $\phi$ . This equation can be conveniently rewritten in terms of the dimensionless quantities  $x = m_\phi/T$  and  $Y_\phi = n_\phi/s$ , where  $s$  is the entropy per comoving volume,  $s = 2\pi^2 g_{*s} T^3/45$ . Assuming a radiation-dominated era, with energy density  $\rho_R = \pi^2 g_* T^4/30$  (here,  $g_* \sim g_{*s} \sim 100$  counts the number of relativistic degrees of freedom) and using that  $Y_\phi \ll Y_{\phi,eq}$  in the large portion of parameter space in which  $\phi$  does not thermalize, one gets:

$$\frac{dY_\phi}{dx} \simeq \frac{\langle\sigma_{AV}\rangle \mathcal{C} m_\phi M_P}{x^2} Y_{\phi,eq}^2, \quad (33)$$

where  $\mathcal{C} = 2\pi\sqrt{90}g_{*s}/(45\sqrt{g_*}) \simeq 13.7$ . For relativistic  $\phi$ ,  $x \ll 1$ , the equilibrium density is approximately given by  $Y_{eq} \sim 0.278/g_{*s}$ . This leads to the approximate formula

$$Y_\phi(T) \sim \epsilon^2 \frac{\Lambda^4}{f^4} \mathcal{C} Y_{\phi,eq}^2 \frac{M_P}{T}. \quad (34)$$

---

<sup>8</sup>Double production can also be mediated by the process  $SM + SM \rightarrow h^{(*)} \rightarrow \phi + \phi$  induced by the  $\phi\phi h$ -coupling, which can lead to a similar thermal production as the one discussed here. Single production, on the other hand, is due to interactions that are linear in the  $\phi$  field and are thus suppressed by the small mixing angle  $\theta_{\phi h}$ , and can be neglected.

<sup>9</sup>This also implies that we can neglect thermal corrections to the potential for  $\phi$  in the analysis of its cosmological evolution.

The  $\phi$  production is maximal at  $T \sim m_h$ . Using Eq. (34) evaluated at  $T \sim m_h$  and assuming no late entropy production, we can deduce, in the parameter region where  $\phi$  is cosmologically stable, the contribution of  $\phi$  to dark matter today,  $\Omega_\phi \sim m_\phi Y_\phi s_0 / \rho_c$  where  $s_0$  is the present entropy density. We find that  $\Gamma_\phi$  is subdominant; for example, along the contour  $\Gamma_\phi = H_0$  in Fig. 3, we have  $\Omega_\phi \lesssim 3 \times 10^{-4}$ , while for  $\Gamma_\phi \simeq 10^{-10} H_0$  we find  $\Omega_\phi \lesssim 7 \times 10^{-11}$ .

### Constraints from BBN and Gamma-Ray observations

As mentioned earlier, there is a region of parameter space in which  $\phi$  is not cosmologically stable and decays after BBN. This is problematic if the decay of  $\phi$  injects into the thermal bath an energy per baryon  $E_{p,b} \gtrsim O(\text{MeV})$ , leading to a modification of the predictions for the abundances of the light elements. Since  $E_{p,b} \sim m_\phi Y_\phi n_\gamma / n_b$ , where  $Y_\phi$  is the abundance prior to decay (i.e. the value of Eq. (34) obtained as if  $\phi$  were stable), this results in the bound  $m_\phi Y_\phi \lesssim 10^{-12} \text{ GeV}$ , which however could be weakened sensitively depending on the precise value of the lifetime [15]. In the parameter space region where  $\phi$  decays between cosmic times  $\sim 1 \text{ s}$  and  $H_0^{-1} \sim 10^{17} \text{ s}$ ,  $m_\phi$  varies from  $\sim 100 \text{ GeV}$  down to  $1 \text{ MeV}$  and  $m_\phi Y_\phi$  varies from  $10^{-2}$  to  $10^{-12} \text{ GeV}$ . Above the di-pion threshold, hadronic decays constrain short lifetimes  $\Gamma_\phi^{-1} \lesssim 10^3 \text{ s}$  while for lighter  $\phi$ , electromagnetic decays constrain large lifetimes  $\gtrsim 10^5 \text{ s}$  [16, 17]. In addition, the Cosmic Microwave Background (CMB) constrains lifetimes  $\sim [10^{10} - 10^{13}] \text{ s}$  for  $E_{p,b}$  down to  $O(\text{eV})$ . Therefore, we expect that most of the region of the parameter space delimited by the lines  $\Gamma_\phi = H_{BBN}$  and  $\Gamma_\phi = H_0$  in Fig. 3 is excluded. A dedicated analysis is however needed to derive the precise excluded regions that is beyond the scope of this paper.

On the other hand, for regions in which the  $\phi$  lifetime is larger than the age of the universe, there are strong constraints coming from decays generating a distortion in the galactic and extra-galactic diffuse X-ray or gamma-ray background. In particular, sub-GeV dark matter decaying into photons should satisfy  $\tau_{DM} \gtrsim 10^{27} \text{ s}$  [18]. Since the gamma-ray flux scales as  $d\Phi_\gamma/dE \propto Y_\phi \Gamma_\phi$ , we can translate this bound into  $\tau_\phi > 10^{27} \text{ s} \times \Omega_\phi / \Omega_{DM}$ . This excludes the thin brown band of Fig. 3.

We stress again that the cosmological constraints derived above can be evaded if the temperature of the universe never reaches  $m_h$ , in which case the thermal production of  $\phi$  is suppressed.

## 6 Conclusion

The aim of this paper has been to provide an existence proof of a model, based on the idea of [4], that can naturally accommodate a small electroweak scale without (sadly, to say) requiring visible new-physics at present and far future colliders. The model is based on a cosmological evolution of the Higgs and two axion-like states whose back-reactions lead to a naturally small electroweak scale. The only new-physics of the model consists of these two scalars,  $\phi$  and  $\sigma$ , that in most of the parameter space are very light and very weakly coupled to the SM. Therefore strategies to detect them are completely different, as they do not require powerful high-energy colliders, but dedicated searches in the sub-GeV regime.

Interestingly, one of the two light states, namely  $\sigma$ , could be a dark matter candidate. Because of its small mass,  $\sigma$  starts oscillating very late and can therefore make a large contribution to dark matter today. The field  $\phi$  cannot contribute to more than  $\Omega_\phi \lesssim 10^{-10}$ . For this maximum value, it may still be detected in gamma-ray observations from its late decay.

Part of the parameter space of our model can be tested through observations of the diffuse gamma-ray backgrounds, black hole superradiance and even in pulsar timing arrays. In addition, there is a rather rich BBN and CMB phenomenology which motivates a more thorough study. Unfortunately, fifth-force signals and Equivalence Principle violations in intermediate mass ranges seem too small to be seen in the near future.

There are important discussions that we leave for the future. An interesting aspect of our mechanism is that it does not depend on initial conditions for the new scalars, provided that it takes place during a long period of inflation. Similarly to [4], we need a very long period of inflation,  $N_e \gtrsim 10^{25}$ , and an inflation scale rather low,  $\lesssim 10^9$  GeV. In addition, inflation requires super-Planckian field excursions. All of these issues deserve further study. It seems clear that the possibility to further increase the effective cutoff  $\Lambda$  might help with these questions.

To close on a more philosophical note, the ideas proposed in [4] and pursued here represent a new twist in the long and fruitful history of the interplay between particle physics and cosmology. While in the past particle physics has been a crucial ingredient to understand the cosmological history of our universe, if these new ideas were correct, cosmological evolution would be a key ingredient in the understanding of some key parameters of particle physics.

## Acknowledgments

We thank Joan Elias-Miró, Eduard Massó and Marc Riembau for very useful discussions in the early stages of this project and David E. Kaplan, Kai Schmidt-Hober and Alexander Westphal for very interesting discussions. We acknowledge support by the Spanish Ministry MEC under grants FPA2014-55613-P, FPA2013-44773-P, and FPA2011-25948, by the Generalitat de Catalunya grant 2014-SGR-1450 and by the Severo Ochoa excellence program of MINECO (grant SO-2012-0234). CG is supported by the European Commission through the Marie Curie Career Integration Grant 631962. CG and GS are supported by the Helmholtz Association. The work of AP has been supported by the Catalan ICREA Academia Program.

## A A partial UV completion of the model

Let us start the discussion by summarizing the basic building blocks of the potential of Eq. (4). The first ingredient is the effective potential for the scalar  $\phi$  that contains two types of terms. The periodic term,<sup>10</sup> associated to a discrete shift invariance,  $\phi \rightarrow \phi + 2\pi f$ , and the linear terms that break this symmetry by the small coupling  $g$ . It is crucial that both types of terms couple to  $|H|^2$  for the CHAIN mechanism to work. Due to Eq. (15), we have  $g \ll \epsilon$  and therefore the linear terms are always smaller than the periodic term. In addition, the model also contains a second field,  $\sigma$ , whose interactions are controlled by the small coupling  $g_\sigma$ , in such a way that  $\sigma$  always appears in the combination  $g_\sigma \sigma / \Lambda$ . In analogy to the  $\phi$  field, we can associate  $\sigma$  to a continuous shift invariance, whose breaking is controlled by  $g_\sigma$ . It is crucial to have a coupling of  $\sigma$  to the periodic function of  $\phi$ , but not a direct coupling to the Higgs that would spoil the CHAIN mechanism, as we mentioned before. Quantum effects via a loop of  $\phi$ -field can of course generate this coupling,  $\sigma |H|^2$ , but its size of order  $O(\epsilon^2 g_\sigma)$  is small enough and does not destabilize the weak scale.

Although each of these terms needs an appropriate UV origin, here we are only interested in providing a UV model that explains the generation of the periodic terms in the potential of Eq. (4). The model is a generalization of the non-QCD model proposed in Section 3 of Ref. [4]. It consists of a gauge sector, which, analogously to QCD, we take to be  $SU(N)$ , with two Dirac fermions,  $L$  and  $N$ , belonging to the fundamental representation of  $SU(N)$ .

---

<sup>10</sup>The form of the periodic function is not important for the model. The choice  $\cos(\phi/f)$  has been selected in view of a possible axion-like UV completion, as we will see in the following.

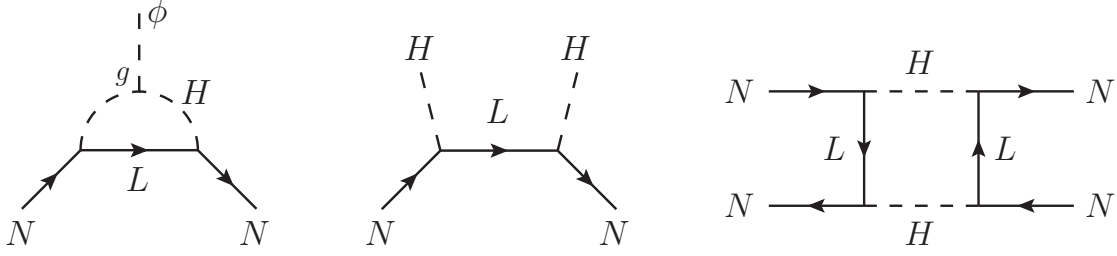


Figure 4: **Left:** Diagram generating  $\phi\bar{N}N$  at the radiative level. **Middle:** Diagram contributing to the coupling  $\bar{N}N|H|^2$ . **Right:** Diagram generating an  $O(\epsilon^2)$  contribution to  $(\bar{N}N)^2$ .

Under the  $SU(2)_L \times U(1)_Y$  SM group,  $L$  has the quantum numbers of a lepton doublet, while  $N$  is a singlet. We assume that the  $SU(N)$  gauge sector becomes strongly-coupled at the scale  $\Lambda$ . A key ingredient of the model is the presence of a specific set of mass and interaction terms for the fermions that break the accidental global symmetries. We assume that the  $L$  and  $N$  fields have Dirac masses (here and in the following we neglect  $O(1)$  parameters):

$$\mathcal{L}_{mass} = \Lambda \bar{L}L + \epsilon \Lambda \bar{N}N, \quad (35)$$

and couplings to the SM Higgs given by

$$\mathcal{L}_{Yuk} = \sqrt{\epsilon} \bar{L}HN + h.c.. \quad (36)$$

Finally, interaction terms of the singlet  $N$  to the  $\sigma$  and  $\phi$  fields are included with couplings of order  $\epsilon g$  and  $\epsilon g_\sigma$  respectively

$$\mathcal{L}_N = \epsilon g \phi \bar{N}N + \epsilon g_\sigma \sigma \bar{N}N. \quad (37)$$

As can be seen from the Lagrangian above, we have associated to each  $N$  field a coupling  $\sqrt{\epsilon} \ll 1$ . In the limit  $\epsilon \rightarrow 0$  the theory acquires an additional chiral invariance (broken only by the axial anomaly). It is interesting to notice that even if we do not introduce in the Lagrangian the coupling of the  $\phi$  field to  $N$ , it is nevertheless generated at the radiative level due to the presence of the  $g\Lambda\phi|H|^2$  coupling in the effective Lagrangian, as shown by the left diagram of Fig. 4.

We also assume that the  $\phi$  field interactions are invariant under a shift-symmetry,  $\phi \rightarrow \phi + c$ , up to the explicit breakings due to  $g$ , and an anomalous interaction term

$$\frac{\phi}{f} G'_{\mu\nu} \tilde{G}'^{\mu\nu}, \quad (38)$$

where  $G'$  denotes the  $SU(N)$  field strength. Analogously to the QCD axion, the field  $\phi$  acquires a periodic effective potential as a consequence of the chiral anomaly. The best way to estimate the size of this contribution is to perform a chiral rotation for  $N$  such that one eliminates the term (38) but generates  $m_N \bar{N}N \rightarrow m_N e^{i\phi/f} \bar{N}N$ , where  $m_N$  is the effective mass of  $N$ :

$$m_N \simeq \epsilon \left( \Lambda + g_\sigma \sigma + g\phi - \frac{|H|^2}{\Lambda} \right), \quad (39)$$

with the last term arising from the middle diagram of Fig. 4. Using  $\langle \bar{N}N \rangle \sim \Lambda^3$ , the term  $m_N e^{i\phi/f} \bar{N}N + h.c.$  gives, at  $O(\epsilon)$ ,

$$V \simeq \Lambda^3 m_N \cos(\phi/f). \quad (40)$$

Equation (40), together with Eq. (39), reproduces the periodic term of Eq. (4).

Using this explicit UV model we can also analyze possible additional contributions to the  $\phi$  potential. For example, at  $O(\epsilon^2)$  we expect contributions to the  $\phi$  potential coming from terms  $(\bar{N}N)^2$  generated at the quantum level from diagrams as the one shown in Fig. 4. After the chiral rotation described above, that eliminates Eq. (38), we have  $(\bar{N}N)^2 \rightarrow (\bar{N}N e^{i\phi/f})^2$ , which leads to a term for the  $\phi$  potential  $\sim \epsilon^2 \Lambda^4 \cos^2(\phi/f)$ . As we discussed in the main text, in order for the relaxation mechanism to work we need to suppress these terms with respect to the leading potential in Eq. (4). This leads to the condition in Eq. (14).

## B Relaxation in a two Higgs doublet scenario

In this appendix we present a relaxation model based on a two Higgs doublet model (2HDM). The motivation for this is, as mentioned in the introduction, to generate the term  $h \cos(\phi/f)$  that requires a second source of EWSB. If the second Higgs is also elementary, we must find a way to keep its mass also small. Otherwise, we expect that, at the end of the relaxation process, only one Higgs being light, while the second doublet having generically a mass of the order  $\Lambda$ .

To solve this problem we can advocate an additional global  $SU(2)_R$  invariance at the scale  $\Lambda$  under which the two Higgses transform as a doublet,  $(H_1, H_2)$ , ensuring that both have the same masses and quartic couplings. This symmetry guarantees that the masses of the two Higgses are canceled simultaneously by the  $\phi$  field. The  $SU(2)_R$  symmetry can be easily extended to the third quark generation sector by considering a type-II 2HDM in which the  $b_R$  and  $t_R$  components form an  $SU(2)_R$ -doublet, and the Yukawa term is given by

$$y \bar{Q}_L (H_1 \ H_2) (b_R \ t_R)^T + h.c.. \quad (41)$$

Below  $\Lambda$ , the most important source of breaking of the  $SU(2)_R$  invariance arises from the SM hypercharge gauge-boson that of course distinguishes  $b_R$  from  $t_R$  (and  $H_1$  from  $H_2$ ).<sup>11</sup> The effective potential involving the Higgses and the field  $\phi$  reads

$$V(H_1, H_2, \phi) = \Lambda^3 g \phi + m_H^2(\phi) (|H_1|^2 + |H_2|^2) + \lambda (|H_1|^2 + |H_2|^2)^2 + \Delta m^2 |H_1|^2 + (\epsilon \Lambda^2 H_1 H_2 e^{i\phi/f} + h.c.) + \dots, \quad (42)$$

where  $m_H^2(\phi) = -\Lambda^2 (1 - g\phi/\Lambda)$ . In the above expression we included the leading  $SU(2)_R$ -breaking  $\Delta m^2 |H_1|^2$ , that arises from two-loop diagrams involving fermions and the hypercharge gauge-boson, and whose size can be estimated to be

$$\Delta m^2 \sim \frac{g'^2 y^2}{(16\pi^2)^2} \Lambda^2. \quad (43)$$

If we want this model to have two independent sources of EWSB,  $H_1$  and  $H_2$ , we encounter a phenomenological problem. The model will contain extra light Higgs, of mass of order  $\lesssim \sqrt{\lambda} v$ , that have not been seen at the LHC. For this reason, we are forced to look for 2HDMs in which only one Higgs,  $H_2$ , is responsible for triggering EWSB, while the other Higgs,  $H_1$ , gets a vacuum expectation value from its mixing with  $H_2$ . The masses of the extra Higgs will then be of order  $\Delta m$  that can be heavier than the EW scale and escape present detection.

The dynamics of this model is quite straightforward to understand. When, as a consequence of the slow-roll of  $\phi$ ,  $m_H^2(\phi)$  becomes negative, only  $H_2$  turns on, as the  $H_1$  mass is still positive if, as we assume from now on,  $m_H^2(\phi) + \Delta m^2 > 0$ . Nevertheless, the periodic term in the potential automatically induces a tadpole for  $H_1$  which displaces it from the origin. In such a scenario we have

$$\langle H_2 \rangle \simeq v, \quad \langle H_1 \rangle \simeq \frac{\epsilon \Lambda^2}{\Delta m^2} v. \quad (44)$$

As the 3rd family Yukawas are equal, Eq. (41), we have  $m_b/m_t \simeq \langle H_1 \rangle / \langle H_2 \rangle$ , that requires

$$\epsilon \Lambda^2 / \Delta m^2 \simeq m_b / m_t. \quad (45)$$

In order for the relaxation mechanism to work, we need to ensure that the potential is radiatively stable. The fact that we have two Higgses helps to protect the periodic term of

---

<sup>11</sup>An additional breaking is induced at one loop by light fermion Yukawas. These effects are however subleading with respect to the ones induced by the hypercharge gauging.



Eq. (42) that can only be self-renormalized. Therefore the only one-loop extra term that we can have is given by

$$\frac{1}{16\pi^2}\epsilon^2\Lambda^4\cos^2(\phi/f), \quad (46)$$

that should be smaller than the periodic term in Eq. (42) (recall that here, contrary to our main model, we are not introducing the field  $\sigma$ ). This leads to the condition

$$\epsilon \lesssim 16\pi^2 \frac{m_b}{m_t} \frac{v^2}{\Lambda^2}, \quad (47)$$

which, together with Eq. (43) and Eq. (45) gives an upper bound on the cut-off  $\Lambda$ :

$$\Lambda \lesssim \frac{(16\pi^2)^{3/2}}{g'y} v \simeq 10^6 \text{ GeV}. \quad (48)$$

This model is thus characterized by three scales: the weak scale  $v$ , the mass of the second Higgs doublet  $m_{H_1} \sim \Delta m \lesssim 10 v$ , and the scale of new dynamics  $\Lambda \lesssim 10^3 v$ . This implies that only the second Higgs doublet would be reachable at the next LHC runs.

## References

- [1] K. G. Wilson and J. B. Kogut, Phys. Rept. **12** (1974) 75.
- [2] G. 't Hooft, NATO Sci. Ser. B **59** (1980) 135.
- [3] M. Dine, [hep-ph/1501.01035].
- [4] P. W. Graham, D. E. Kaplan and S. Rajendran, [hep-ph/1504.07551].
- [5] L. F. Abbott, Phys. Lett. B **150** (1985) 427.
- [6] G. Dvali and A. Vilenkin, Phys. Rev. D **70**, 063501 (2004) [[hep-th/0304043](#)].
- [7] G. Dvali, Phys. Rev. D **74**, 025018 (2006) [[hep-th/0410286](#)].
- [8] J. R. Espinosa, G. F. Giudice and A. Riotto, JCAP **0805** (2008) 002 [hep-ph/0710.2484];  
J. R. Espinosa et al., [hep-ph/1505.04825].
- [9] J. R. Ellis, M. K. Gaillard and D. V. Nanopoulos, Nucl. Phys. B **106** (1976) 292.
- [10] F. Bezrukov and D. Gorbunov, JHEP **1005** (2010) 010 [hep-ph/0912.0390].

- [11] K. Schmidt-Hoberg, F. Staub and M. W. Winkler, Phys. Lett. B **727** (2013) 506 [[hep-ph/1310.6752](#)].
- [12] J. D. Clarke, R. Foot and R. R. Volkas, JHEP **1402** (2014) 123 [[hep-ph/1310.8042](#)].
- [13] G. F. Giudice, E. W. Kolb and A. Riotto, Phys. Rev. D **64**, 023508 (2001) [[hep-ph/0005123](#)].
- [14] A. Arvanitaki, M. Baryakhtar and X. Huang, Phys. Rev. D **91**, no. 8, 084011 (2015) [[hep-ph/1411.2263](#)].
- [15] R. H. Cyburt, J. R. Ellis, B. D. Fields and K. A. Olive, Phys. Rev. D **67**, 103521 (2003) [[astro-ph/0211258](#)].
- [16] H. An, M. Pospelov, J. Pradler and A. Ritz, Phys. Lett. B **747**, 331 (2015) [[hep-ph/1412.8378](#)].
- [17] M. Kawasaki, K. Kohri and T. Moroi, Phys. Rev. D **71**, 083502 (2005) [[astro-ph/0408426](#)].
- [18] R. Essig, E. Kuflik, S. D. McDermott, T. Volansky and K. M. Zurek, JHEP **1311** (2013) 193 [[hep-ph/1309.4091](#)].
- [19] A. Khmelnitsky and V. Rubakov, JCAP **1402**, 019 (2014) [[astro-ph.CO/1309.5888](#)].
- [20] R. Hlozek, D. Grin, D. J. E. Marsh and P. G. Ferreira, Phys. Rev. D **91** (2015) 10, 103512 [[astro-ph.CO/1410.2896](#)].